Nonlinear optical absorption and optically detected electrophonon resonance in GaAs based $n − i − p − i$ superlattices

Nguyen T. Dung [a], Vo T.T. Vi [b],[*], Le T.T. Phuong [c],[d],[**]

[a] Vinh University, Nghe An, Viet Nam
[b] Faculty of Basic Sciences, Hue University of Medicine and Pharmacy, Hue University, Hue, Viet Nam
[c] Center for Theoretical and Computational Physics, University of Education, Hue University, Hue, Viet Nam
[d] Department of Physics, University of Education, Hue University, Hue, Viet Nam

ARTICLE INFO

ABSTRACT

The quantisation of electronic energy into subbands in low-dimensional structures originates many interesting physical effects, one of which is the electrophonon resonance effect. In this work, we investigate the electrophonon resonance by theoretically calculating the optical absorption power in $n − i − p − i$ superlattices (SLs) subjected to a high frequency electromagnetic wave. The absorption power is calculated up to the first-order nonlinear term using the projection operator technique taking account of the effect of electron – optical phonon interaction. Numerical results are obtained and discussed for the GaAs:Si/GaAs:Be SL. The linear and nonlinear optically detected electrophonon resonance (ODEPR) peaks are observed in the absorbance. The full width at half maximum (FWHM) of ODEPR peaks increases with increasing the doping concentration as well as temperature. In particular, the results show that the two-photon absorption is of great importance and should be considered in nonlinear optics. This investigation provides a theoretical basis for potential applications of $n − i − p − i$ SLs in optoelectronic devices.

1. Introduction

Quasi-two-dimensional semiconductor superlattices (SLs) are the artificial structures in which charged carriers are confined in one direction by a superlattice potential with the period being longer than the lattice constant and shorter than the mean free path of electrons. This superlattice potential was first proposed by Esaki and Tsu [1] by alternatively arranging, in a periodic sequence, ultrathin layers of semiconductors of different types or by alternatively doping impurities into a intrinsic semiconductor, or by a combination of alternating composition and alternating doping. The first and the second technique give us, respectively, the so-called *compositional* and $n − i − p − i$ (or *doping*) superlattice. While the former requires a close lattice match of the component materials, the relatively small amount of doping in the latter results to only a minor distortion of the lattice of the host material. Practically, the SL potential and SL period are tuneable by changing the compositions or the doping concentration. In addition, the splitting of the valence and conduction bands into subbands (minibands) in SLs makes their energy dispersion completely different in comparison with the doped monolayer materials [2–5]. It is also the origin of many interesting physical properties in SLs [6–8], one of them is the

electrophonon resonance effect. In addition, it was shown that $n - i - p - i$ superlattices exhibit very unusual nonlinear optical properties [6] and their optical properties are expected to be fairly different from those in monolayer 2D materials [9–18].

Electrophonon resonance effect occurs in a low-dimensional electron system when electrons move between energy subbands by absorbing/emitting optical phonons whose energy is equal to the energy difference of the two subbands [19–22]. When an additional electromagnetic wave (EMW) propagates in the system, we can observe the so-called optically detected electrophonon resonance (ODEPR) effect when electron transitions via absorbing and/or emitting phonons and photons satisfy the selection rules $\hbar\omega = \Delta E_{\text{subbands}} \pm \hbar\omega_{\text{oph}}$, where $\hbar\omega$, $\hbar\omega_{\text{oph}}$, and $\Delta E_{\text{subbands}}$ are, respectively, the photon energy, the optical phonon energy, and the energy difference between two electronic subbands. Based on the absorption spectrum, many applications could be proposed such as probing the carrier effective mass, the phonon energy, the distance between energy subbands, and so on. Up to date, there have been numerous researches dealing with the optical transport properties as well as electrophonon resonance in low-dimensional structures [23–26]. To our knowledge, the optical transport properties in $n - i - p - i$ SLs, taking account of the carrier – phonon interaction still remain problems to study. In SLs the interesting quantisation of electronic energy into subbands which can be adjusted by the SL's parameters, is expected to result in fascinating behaviours of the optical tranport. In this work, we theoretically investigate the optical absorption in a GaAs based $n - i - p - i$ semiconductor SL stimulated by a high frequency EMW. Within this work, we only consider high temperature range when the electron – optical phonon interaction is dominant and taken into account. We derive an analytical expression for the absorption power (AP) including linear and nonlinear terms. The analytical result is numerically evaluated and analysed for the GaAs: Si/GaAs:Be SL. The dependence of the absorption characteristics on the external fields, temperature of the system, and the doping concentration is shown clearly. The paper is structured as follows. In the next section (Sec. 2), we present briefly the theoretical model and the derivation of the AP. Numerical results and discussion are given in Sec. 3. Finally, important conclusions are given in Sec. 4.

2. Theoretical model and analytical results

We consider a $n - i - p - i$ superlattice (SL) in which the *intrinsic*, n-doped, and p-doped semiconductor layers are grown alternatively and periodically in the z-direction by the order shown in Fig. 1. Charged carriers in the structure are then free in the (x, y) plane and their motion in the z-direction is governed by the superlattice potential of period d. In a simple model suggested by K. Ploog and G. H. Dohler [27], the SL can be considered as a multiple-quantum well structure in which the confinement potential in each individual well is idealised to be parabolic. In most cases of interest it is justified to neglect the interaction between neighbouring potential wells. Then, the one-particle wave function and corresponding energy of an electron in an individual potential well are, respectively, given by [27].

$$\Psi(\overrightarrow{r}) \equiv |\alpha\rangle = \frac{1}{\sqrt{L_x L_y}} e^{\overrightarrow{r}_{\perp} \overrightarrow{k}_{\perp}} \varphi_{n_\alpha}(z), \tag{1}$$

$$E_{n_\alpha}(k_\perp) \equiv E_\alpha = \frac{\hbar^2 (\overrightarrow{k}_{\perp}^{\alpha})^2}{2m^\star} + \left(n_\alpha + \frac{1}{2}\right)\omega_p, \tag{2}$$

where $\overrightarrow{k}_{\perp} = (k_x, k_y)$ is the electron wave vector in the (x, y) plane; L_x and L_y are the normalisation length in the x- and y-direction, respectively; $\varphi_{n_\alpha}(z)$ ($n_\alpha = 0, 1, 2, \ldots$) is the eigenfunction of an electron in a potential well; $m^\star$ is the electron effective mass; $\omega_p = \left(\frac{4\pi e^2 n_D}{\varepsilon m^\star}\right)^{1/2}$ is the plasma frequency characterising for the superlattice confinement potential with e being the electronic charge; n_D the doping concentration and ε the dielectric constant.

When an intense EMW (optical field) of amplitude E_0 and frequency ω propagates in the SL, the optical transport property in the system can be investigated via the AP. The total AP, $P(\omega)$, is determined by the direct relation with the optical conductivity, $\sigma(\omega)$, as [28,29].
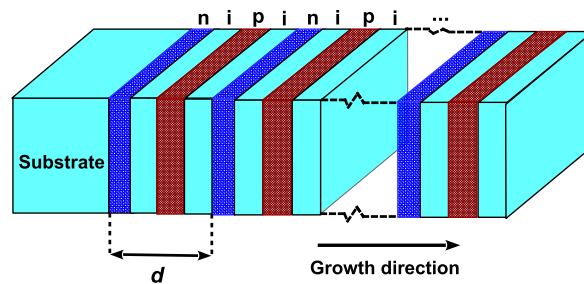

Fig. 1. (Color online) An illustration of a $n - i - p - i$ SL in which a sample of intrinsic semiconductor (*i*) is doped alternatively and periodically by negative charged (*n*) and positive charged (*p*) impurities in one direction (the growth direction). (For interpretation of the references to colour in this figure legend, the reader is referred to the Web version of this article.)

$$P(\omega) = \frac{E_0^2}{2} \mathcal{R}e\{\sigma(\omega)\}, \tag{3}$$

where "$\mathcal{R}e$" denotes "the real part of". In this calculation, we consider the optical conductivity up to two-photon absorption processes. The optical conductivity can be deduced using the technique introduced by Lee et al. [30] from the ensemble average of the current density operator [31].

$$
\begin{aligned}
\langle J_i \rangle_{ens} &= \sum_{j=1}^{3} \sigma_{ij}(\omega) E_j(\omega) + \sum_{j,k=1}^{3} \sigma_{ijk}(\omega_1, \omega_2) E_j(\omega_1) E_k(\omega_2) \\
&= \left[\sum_{j=1}^{3} \sigma_{ij}(\omega) + \sum_{j,k=1}^{3} \sigma_{ijk}(\omega_1, \omega_2) E_k(\omega_2) \right] E_j(\omega),
\end{aligned}
\tag{4}
$$

where J_i is the ith current component, $i, j, k \equiv x, y, z$. The first and the second term in the square bracket of Eq. (4) are referred, respectively, as the linear and the lowest-order nonlinear conductivity tensor where the nonlinear one includes the processes of the absorption of two photons with frequencies ω_1 and ω_2. In this investigation, we consider only one EMW of frequency ω. Therefore the two absorbed photons have the same frequencies, i. e. $\omega_1 = \omega_2 = \omega$, followed by the expression for the total optical conductivity deduced from Eq. (4)

$$\sigma(\omega) = \sigma_{ij}(\omega) + \sum_{k=1}^{3} \sigma_{ijk}(\omega) E_k(\omega). \tag{5}$$

Assuming that the electromagnetic wave polarises in the z-direction, i.e. $E_z(\omega) = E_0 e^{i\omega t}$, the AP delivered to the system of electrons interacting with phonons in the SL is then given by

$$
\begin{aligned}
P(\omega) &= \frac{E_0^2}{2} \mathcal{R}e\{\sigma_{zz}(\omega)\} + \frac{E_0^2}{2} \mathcal{R}e\{\sigma_{zzz}(\omega) E_z(\omega)\} \\
&\equiv P^{(0)}(\omega) + P^{(1)}(\omega),
\end{aligned}
\tag{6}
$$

where we have set $P^{(0)}(\omega) = (E_0^2/2)\mathcal{R}e\{\sigma_{zz}(\omega)\}$ and $P^{(1)}(\omega) = (E_0^2/2)\,\mathcal{R}e\{\sigma_{zzz}(\omega) E_z(\omega)\}$ which are referred as the linear and nonlinear term of the total AP, respectively. To obtain the explicit expression of the AP, one need to calculate the conductivities $\sigma_{zz}(\omega)$ and $\sigma_{zzz}(\omega)$ which are presented as follows for the case of electron – optical phonon interaction.

2.1. The linear conductivity

Utilizing the general expression for the conductivity presented by Lee et al. [30] and Kang *el al.* [31], the linear conductivity in the SL is given by

$$\mathcal{R}e\{\sigma_{zz}(\omega)\} = e \sum_{\alpha,\beta} (z^{\alpha,\beta})(j_z^{\alpha,\beta}) \frac{(f_\beta - f_\alpha) B_0^{\alpha,\beta}(\omega)}{[\hbar\omega - E_{\beta,\alpha}]^2 + [B_0^{\alpha,\beta}(\omega)]^2}. \tag{7}$$

Here, $E_{\beta,\alpha} = E_\beta - E_\alpha$; E_α and E_β is the energy of the electron in the initial and final state, respectively; f_α is the Fermi-Dirac distribution function of electron with energy E_α; $z^{\alpha,\beta}$, $j_z^{\alpha,\beta}$, and $B_0^{\alpha,\beta}(\omega)$ [30,31] are the component of the electron position vector, the matrix element of the current operator, and the linewidth function, respectively, which are calculated as

$$z^{\alpha,\beta} = \frac{\ell_z}{\sqrt{2}} \left(\sqrt{n_{\alpha+1}} \, \delta_{n_\beta, n_\alpha+1} + \sqrt{n_\alpha} \, \delta_{n_\beta, n_\alpha-1} \right) \delta_{k_\perp^\alpha, k_\perp^\beta}; \quad \ell_z = \hbar^{1/2}(m^\star \omega_p)^{-1/2}, \tag{8}$$

$$
j_z^{\alpha,\beta} =
\begin{cases}
\left(\dfrac{e\hbar n_\beta}{m^\star L_z} \right)^{1/2} \left[\dfrac{(-1)^{n_\alpha+n_\beta} - 1}{n_\alpha + n_\beta} + \dfrac{(-1)^{n_\alpha-n_\beta} - 1}{n_\alpha - n_\beta} \right] \delta_{k_\perp^\alpha, k_\perp^\beta}, & n_\beta \neq n_\alpha, \\
0, & n_\beta = n_\alpha,
\end{cases}
$$

$$
\begin{aligned}
B_0^{\alpha,\beta}(\omega) &= \frac{\pi}{(f_\beta - f_\alpha)} \sum_{q,\nu} |C_{\beta\nu}(q)|^2 \left\{ \left[(1 + N_q) f_\alpha (1 - f_\nu) - N_q f_\nu (1 - f_\alpha) \right] \delta(Y_1^-) \right. \\
&\quad + \left. \left[N_q f_\alpha (1 - f_\nu) - (1 + N_q) f_\nu (1 - f_\alpha) \right] \delta(Y_1^+) \right\} \\
&\quad + \frac{\pi}{(f_\beta - f_\alpha)} \sum_{q,\nu} |C_{\alpha\nu}(q)|^2 \left\{ \left[(1 + N_q) f_\nu (1 - f_\beta) - N_q f_\beta (1 - f_\nu) \right] \delta(Y_2^-) \right. \\
&\quad + \left. \left[N_q f_\nu (1 - f_\beta) - (1 + N_q) f_\beta (1 - f_\nu) \right] \delta(Y_2^+) \right\},
\end{aligned}
\tag{9}
$$

where δ is the delta function, N_q is the Plank distribution for a phonon in the state $|q\rangle$, and

$$Y_1^\pm = \hbar\omega - E_{\nu,\alpha} \pm \hbar\omega_q, \quad Y_2^\pm = \hbar\omega - E_{\beta,\nu} \pm \hbar\omega_q. \tag{10}$$

The physical interpretation is clear. The first term in Eq. (9) represents the transition of an electron from state $|\alpha\rangle$ to state $|\nu\rangle$ with a phonon emission. The rest terms can be explained in a similar manner. The electron – phonon interaction matrix element $C_{\alpha\nu}(q)$ is given by [32,33].

$$|C_{\alpha\nu}(q)|^2 = |V(q)|^2 |I_{n_\alpha,n_\nu}(q_z)|^2 \delta_{k_\perp^\alpha, k_\perp^\nu + q_\perp}, \tag{11}$$

where $I_{n_\alpha,n_\nu}(q_z)$ is the form factor or the overlap integral given by

$$I_{n_\alpha,n_\nu}(\pm q_z) = \sum_{j=1}^{s_0} \int_0^d \exp(\pm iq_z d)\varphi_{n_\alpha}(z-jd)\varphi_{n_\nu}(z-jd)dz, \tag{12}$$

with s_0 being the number of periods of the SL and q_z the wave number of phonon in the z-direction. The real and imaginary parts of $I_{n,n'}(q_z)$ are demonstrated in Fig. 2 for several values of quantum numbers n and n'. The electron – phonon interacting potential, V_q, for polar optical phonon with energy $\hbar\omega_0$ has the form

$$|V(q)|^2 = \frac{\Theta}{\Omega q^2}, \tag{13}$$

where $\Theta = 2\pi e^2 \hbar\omega_0(\chi_\infty^{-1} - \chi_0^{-1})/\epsilon_0$; ϵ_0 is the permittivity of free space; χ_∞ and χ_0 are, respectively, the high-frequency and static dielectric constants; and Ω is the volume of the material.

To calculate explicitly $\text{Re}\{\sigma_{zz}(\omega)\}$, we need to calculate $B_0^{\alpha,\beta}(\omega)$ given by Eq. (9) by transforming the summations over q and $|\nu\rangle$ into integrals. After some straight-forward manipulation, we have

$$
\begin{aligned}
B_0^{\alpha,\beta}(\omega) = {} & \frac{m^\star \Theta}{8\hbar^2\pi^2(f_\beta - f_\alpha)}\sum_{n_\nu} A_{n_\beta,n_\nu} \\
& \times \left\{ \frac{k_{1(-)}}{|k_{1(-)}|(k_\perp^\beta - k_{1(-)})}\left[\left(1+N_q\right)f_\alpha(1-f_{n_\nu,k_{1(-)}}) - N_q f_{n_\nu,k_{1(-)}}(1-f_\alpha)\right] \right. \\
& \left. + \frac{k_{1(+)}}{|k_{1(+)}|(k_\perp^\beta - k_{1(+)})}\left[N_q f_\alpha(1-f_{n_\nu,k_{1(+)}}) - (1+N_q)f_{n_\nu,k_{1(+)}}(1-f_\alpha)\right] \right\} \\
& + \frac{m^\star \Theta}{8\hbar^2\pi^2(f_\beta - f_\alpha)}\sum_{n_\nu} A_{n_\alpha,n_\nu} \\
& \times \left\{ \frac{k_{2(-)}}{|k_{2(-)}|(k_\perp^\alpha - k_{2(-)})}\left[\left(1+N_q\right)f_{n_\nu,k_{2(-)}}(1-f_\beta) - N_q f_\beta(1-f_{n_\nu,k_{2(-)}})\right] \right. \\
& \left. + \frac{k_{2(+)}}{|k_{2(+)}|(k_\perp^\alpha - k_{2(+)})}\left[N_q f_{n_\nu,k_{2(+)}}(1-f_\beta) - (1+N_q)f_\beta(1-f_{n_\nu,k_{2(+)}})\right] \right\}
\end{aligned}
\tag{14}
$$

where

$$k_{1(\pm)} = \left\{(k_\perp^\alpha)^2 + \frac{2m}{\hbar^2}\left[\hbar(\omega \pm \omega_0) - \Delta E_{n_\nu,n_\alpha}\right]\right\}^{1/2},$$

$$k_{2(\pm)} = \left\{(k_\perp^\beta)^2 - \frac{2m}{\hbar^2}\left[\hbar(\omega \pm \omega_0) - \Delta E_{n_\beta,n_\nu}\right]\right\}^{1/2},$$
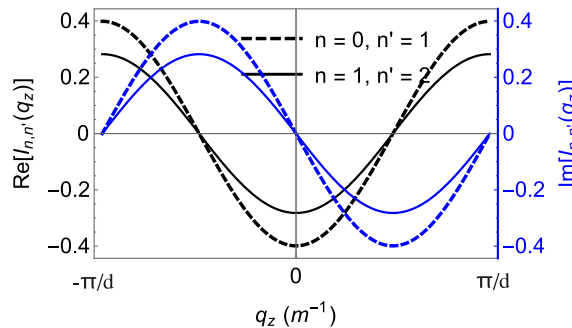

Fig. 2. The real part and imaginary part of the form factor for several subband indices. Here, $d = 50$ nm and $s_0 = 100$.

$\Delta E_{n_\nu,n_\alpha} = (n_\nu - n_\alpha)\hbar\omega_p$ and $A_{n_\alpha,n_\nu} = \int_0^\infty |I_{n_\alpha,n_\nu}(\pm q_z)|^2 dq_z$, which can be numerically evaluated.

2.2. The nonlinear conductivity

The nonlinear conductivity component, $\sigma_{zzz}(\omega)$, can be derived using the general formula obtained by Lee et al. in Ref. [30] [see Eq. (4.19) therein] and given as

$$
\begin{aligned}
\mathrm{Re}\{\sigma_{zzz}(\omega)\} &= e^2 \sum_{\alpha,\beta} z^{\alpha,\beta} \frac{(f_\beta - f_\alpha)}{[\hbar\omega - E_{\beta,\alpha}]^2 + [B_0^{\alpha,\beta}(\omega)]^2} \\
&\times \left\{ \sum_\nu \frac{z^{\nu,\alpha} j_z^{'\beta,\nu}}{[2\hbar\omega - E_{\beta,\nu}]^2 + [B_1^{\alpha,\beta,\nu}(\omega)]^2} \left[(\hbar\omega - E_{\beta,\alpha})B_1^{\alpha,\beta,\nu}(\omega) + (2\hbar\omega - E_{\beta,\nu})B_0^{\alpha,\beta}(\omega) \right] \right. \\
&\left. + \sum_\delta \frac{z^{\beta,\delta} j_z^{'\delta,\alpha}}{[2\hbar\omega - E_{\delta,\alpha}]^2 + [B_2^{\alpha,\beta,\delta}(\omega)]^2} \left[(\hbar\omega - E_{\beta,\alpha})B_2^{\alpha,\beta,\delta}(\omega) + (2\hbar\omega - E_{\delta,\alpha})B_0^{\alpha,\beta}(\omega) \right] \right\},
\end{aligned}
\tag{15}
$$

where

$$
\begin{aligned}
B_1^{\alpha,\beta,\nu}(\omega) &= \frac{\pi}{(f_\beta - f_\alpha)} \sum_{q,\mu} |C_{\nu\mu}(q)|^2 \Big\{ \big[(1+N_q)f_\beta(1-f_\mu) - N_q f_\mu(1-f_\beta) \big] \delta(Y_3^+) \\
&+ \big[N_q f_\beta(1-f_\mu) - (1+N_q)f_\mu(1-f_\beta) \big] \delta(Y_3^-) \Big\} \\
&+ \big[(1+N_q)f_\mu(1-f_\alpha) - N_q f_\alpha(1-f_\mu) \big] \delta(Y_4^-) \\
&+ \big[N_q f_\mu(1-f_\alpha) - (1+N_q)f_\alpha(1-f_\mu) \big] \delta(Y_4^+) \Big\} \\
&+ \frac{\pi}{(f_\beta - f_\alpha)} \sum_{q,\mu} |C_{\mu\beta}(q)|^2 \Big\{ \big[(1+N_q)f_\mu(1-f_\alpha) - N_q f_\alpha(1-f_\mu) \big] \delta(Y_5^+) \\
&+ \big[N_q f_\mu(1-f_\alpha) - (1+N_q)f_\alpha(1-f_\mu) \big] \delta(Y_5^-) \Big\},
\end{aligned}
\tag{16}
$$

with

$$
Y_3^\pm = 2\hbar\omega - E_{\beta,\mu} \pm \hbar\omega_q, \quad Y_4^\pm = 2\hbar\omega - E_{\alpha,\mu} \pm \hbar\omega_q, \quad Y_5^\pm = 2\hbar\omega - E_{\mu,\alpha} \pm \hbar\omega_q.
\tag{17}
$$

The term $B_2^{\alpha,\beta,\delta}(\omega)$ can be obtained from $B_1^{\alpha,\beta,\nu}(\omega)$ by replacing the state index ν by δ.

It is seen that the first-order nonlinear conductivity is much more complicated than the linear one. The physical interpretation of each term in the above expressions has been analysed in detail in Refs. [30,31]. To obtain the explicit expression of $\sigma_{zzz}(\omega)$ and accordingly the AP, we need to perform the same calculations for $B_1^{\alpha,\beta,\nu}(\omega)$ and $B_2^{\alpha,\beta,\delta}(\omega)$ like we have done for $B_0^{\alpha,\beta}(\omega)$ above. For instance, for $B_1^{\alpha,\beta,\nu}(\omega)$ one has

$$
\begin{aligned}
B_1^{\alpha,\beta,\nu}(\omega) &= \frac{\Theta m^\star}{8\hbar^2\pi^2(f_\beta - f_\alpha)} \sum_{n_\mu} A_{n_\nu,n_\mu} \\
&\times \left\{ \frac{k_{3(+)}}{|k_{3(+)}|(k_\perp^\nu - k_{3(+)})} \left[(1+N_q)f_\beta(1-f_{n_\mu,k_{3(+)}}) - N_q f_{n_\mu,k_{3(+)}}(1-f_\beta) \right] \right. \\
&+ \frac{k_{3(-)}}{|k_{3(-)}|(k_\perp^\nu - k_{3(-)})} \left[N_q f_\beta(1-f_{n_\mu,k_{3(-)}}) - (1+N_q)f_{n_\mu,k_{3(-)}}(1-f_\beta) \right] \\
&+ \frac{k_{4(-)}}{|k_{4(-)}|(k_\perp^\nu - k_{4(-)})} \left[(1+N_q)f_{n_\mu,k_{4(-)}}(1-f_\alpha) - N_q f_\alpha(1-f_{n_\mu,k_{4(-)}}) \right] \\
&\left. + \frac{k_{4(+)}}{|k_{4(+)}|(k_\perp^\nu - k_{4(+)})} \left[N_q f_{n_\mu,k_{4(+)}}(1-f_\alpha) - (1+N_q)f_\alpha(1-f_{n_\mu,k_{4(+)}}) \right] \right\} \\
&+ \frac{m^\star\Theta}{8\hbar^2\pi^2(f_\beta - f_\alpha)} \sum_{n_\mu} A_{n_\mu,n_\beta} \\
&\times \left\{ \frac{k_{5(+)}}{|k_{5(+)}|(k_\perp^\beta - k_{5(+)})} \left[(1+N_q)f_{n_\mu,k_{5(+)}}(1-f_\alpha) - N_q f_\alpha(1-f_{n_\mu,k_{5(+)}}) \right] \right. \\
&\left. + \frac{k_{5(-)}}{|k_{5(-)}|(k_\perp^\beta - k_{5(-)})} \left[N_q f_{n_\mu,k_{3(-)}}(1-f_\alpha) - (1+N_q)f_\alpha(1-f_{n_\mu,k_{5(-)}}) \right] \right\},
\end{aligned}
\tag{18}
$$

where

$$k_{3(\pm)} = \left\{ (k_\perp^\beta)^2 + \frac{2m}{\hbar^2} \left[\hbar(2\omega \pm \omega_0) - \Delta E_{n_\beta, n_\mu} \right] \right\}^{1/2},$$

$$k_{4(\pm)} = \left\{ (k_\perp^\alpha)^2 - \frac{2m}{\hbar^2} \left[\hbar(2\omega \pm \omega_0) - \Delta E_{n_\alpha, n_\mu} \right] \right\}^{1/2},$$

$$k_{5(\pm)} = \left\{ (k_\perp^\alpha)^2 + \frac{2m}{\hbar^2} \left[\hbar(2\omega \pm \omega_0) - \Delta E_{n_\mu, n_\alpha} \right] \right\}^{1/2}.$$

The above obtained results have a relatively verbose form. However, physical meanings can be derived from them by performing the numerical computation which we will carry out in the next section.

3. Numerical results and discussion

This session aims to clarify the behaviours of the absorption spectrum with the variation of the external EMW, the temperature, and the doping concentration. To do this, we consider the GaAs:Si/GaAs:Be $n - i - p - i$ SL with the following parameters [27,34,35]: $m^\star = 0.067 m_0$ (m_0 is the mass of free electron), $\hbar\omega_0 = 36.25$ meV, $\chi_\infty = 10.9$, $\chi_0 = 12.9$, $s_0 = 100$, and $d = 50$ nm. The doping concentration will be varied to show its effect on the absorbance.

In Fig. 3 we show the linear term of the total AP as a function of the photon energy at two values of the doping concentration. We can see clearly in the figure the appearance of absorption peaks at some certain values of the photon energy. The physical significance of these peaks can be analysed as follows. On the solid curve, the first peak is located at the photon energy of 36.25 meV, satisfying the condition $\hbar\omega = \hbar\omega_0$. This peak describes the intra-subband transition of an electron by absorbing/emitting an optical phonon accompanied by emitting/absorbing an electromagnetic wave photon with energy being equal to the optical phonon energy. The second and the fourth peaks, respectively, arise at the photon energy of 124.507 meV and 197.007 meV. These peaks correspond to the resonance conditions $\hbar\omega = \Delta E_{2,1} - \hbar\omega_0$ and $\hbar\omega = \Delta E_{2,1} + \hbar\omega_0$, respectively, where $\Delta E_{2,1} = 160.757$ meV. Thus, they are the optically detected electron-phonon resonance peaks in which an electron transit between two different subbands by absorbing/emitting an optical phonon while simultaneously emitting/absorbing a photon. The third peak appears at the photon energy of 160.757 meV satisfying $\hbar\omega = \Delta E_{2,1}$. The meaning of the peaks on the dashed curve can be explained similarly. It should be noted that for the inter-subband transitions, since the energy difference between the two subbands depends on the doping concentration through the plasma frequency, i.e. $\Delta E_{n_\beta, n_\alpha} = (n_\beta - n_\alpha)\hbar\omega_p$, when the doping concentration changes, the photon energy satisfying the resonance condition also changes. This is shown by the shifting of the second, the third and the fourth resonance peaks as varying the doping concentration. On the contrary, because the electron subbands are identical for intra-subband transitions, the resonance energy corresponding to these transitions does not change with the change of the doping concentration as proven by the first peak of the curves in Fig. 3.

The nonlinear term of the AP is also plotted and shown in Fig. 4. We also see the appearance of resonance peaks, similar to that for the linear term. However, in this case there are more in number of resonance peaks in the same photon energy range. Besides the resonance peaks appearing at the photon energy values as in the linear case, there are additional resonance peaks at other values of the photon energy. This can be explained as follows. The resonance peaks arise from the resonance scattering of electrons with photon and phonon satisfying the energy conservation law, which is guaranteed by the delta functions in the expressions of the conductivities in Eqs. (7) and (15). It is seen that for the nonlinear conductivity, and followed by the nonlinear AP term, there are more delta functions than for linear term, so the nonlinear term has more resonance peaks. A special point to note is that in the nonlinear term in Fig. 4, there are resonance peaks coming from the two-photon absorption processes in addition. They are the first and the third peaks in the absorption spectrum that locate, respectively, at the photon energies of 18.125 meV and 80.3786 meV and satisfy the conditions $2\hbar\omega =$
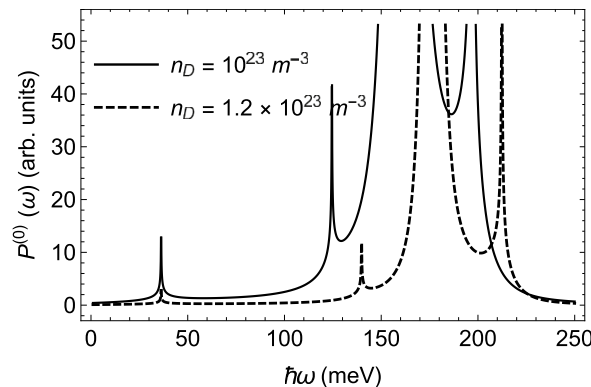

Fig. 3. The linear part of the absorption power as a function of the photon energy. Here, $T = 200$K.

$\hbar\omega_0$ and $2\hbar\omega = \Delta E_{2,1}$. It is clear that the two-photon absorption process has a minor contribution to the absorption spectrum but is observable and cannot be ignored when investigating nonlinear optical effects.

It is well known that the full width at half maximum (FWHM) of resonance peaks has an important role in spectroscopy. Thus, from the graphs for the AP we will computationally extract the FWHM of some resonance peaks and examine its variation with the doping concentration and temperature. The dependence of FWHM on the doping concentration is obtained and shown in Fig. 5 for both one-photon and two-photon absorption precesses. It is seen that the FWHM increases as increasing the doping concentration. The best fit gives us the laws FWHM[meV] $= 0.70n_D[\text{m}^{-3}]$ and FWHM[meV] $= 0.51n_D[\text{m}^{-3}]$ for the one-photon and two-photon case, respectively. The increase of the FWHM with the doping concentration is reasonable because the plasma frequency characterising the carrier confinement increases as the doping concentration increases. This behaviour is in agreement with those observed in low-dimensional electron systems such as quantum wells [25,29] and quantum wires [23,24,26] when the carrier confinement potential is enhanced by reducing the confinement length (the well's width or the wire's radius). The temperature-dependent FWHM is also obtained and shown in Fig. 6(a) and (b) for one-photon and two-photon absorption, respectively. Because the electron – optical phonon interaction is dominant at relatively high temperatures so here we consider the temperature range from 120 K to 350 K. From Fig. 6(a) we can see that the FWHM depends strongly on the temperature. The fitting result gives the dependence as FWHM[meV] $= 0.246 + 0.00076T + 7.04545 \times 10^{-6}T^2$ where T is measured in Kelvin. For the case of two-photon absorption, the FWHM depends rather weakly on T. The evolution of the FWHM can be viewed in two regions of temperature. In the temperature range from 120 K to approximately 235 K, the FWHM increases linearly by the law FWHM[meV] $= 0.422 + 0.000223T$. For the temperature range above 250 K, the FWHM depends very weakly on temperature by the law FWHM[meV] $= 0.455 + 0.00009T$. Qualitatively, the increase of FWHM with temperature is consistent with previous observations in low-dimensional systems such as semiconductor quantum wells [25,29] and quantum wires [23,24,26]. However, unfortunately there have been no experiments on this subject in the $n - i - p - i$ structure to date, further experimental measurements are needed for a quantitative comparison with the our present result.

4. Conclusions

So far, we have calculated the nonlinear optical absorption power in GaAs based $n - i - p - i$ SL taking account of the electron – optical phonon interaction. Numerical results have been obtained for the GaAs:Si/GaAs:Be SL. The linear and nonlinear ODEPR peaks have been observed in the absorbance as expected. The FWHM of ODEPR peaks increases with increasing the doping concentration, i.e. the carrier confinement strength. This behaviour is reasonable and in accordance with those observed before in some low-dimensional structures such as quantum wells and quantum wires in which the FWHM also increases with enhancing the carrier confinement. Also, it can be inferred from this feature that the stronger the confinement, the stronger the electron – phonon interaction. Besides, the FWHM has been found to increase with increasing the temperature in both linear and nonlinear cases. Importantly, the results show that the two-photon absorption plays a considerable role in the absorbance. The obtained results are the basis for further applications in optoelectronic devices. In addition, one can do similar investigations for different kinds of electron – phonon interaction as well as considering the phonon confinement effect.

Author contributions

N.T. Dung: Investigation, Formal analysis, Writing and Editing, Conceptualization. V.T.T. Vi: Software, Formal analysis, Writing and Editing. L.T.T. Phuong: Conceptualization, Methodology, Investigation, Formal analysis, Writing and Editing.

Declaration of competing interest

The authors declare that they have no known competing financial interests or personal relationships that could have appeared to influence the work reported in this paper.
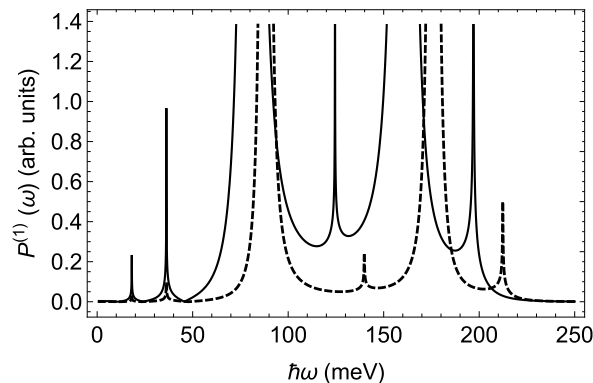

Fig. 4. The nonlinear part of the absorption power versus photon energy. The parameters used in this figure are the same as in Fig. 3.
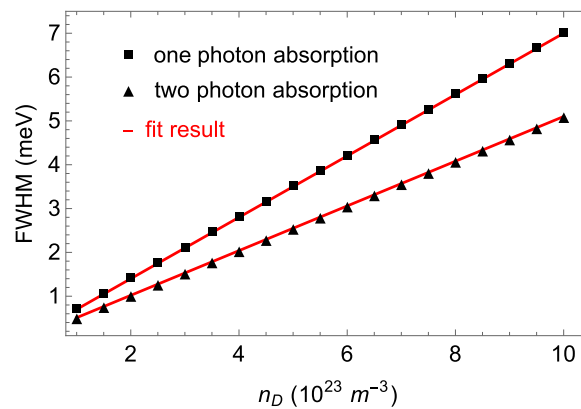
Fig. 5. The dependence of the FWHM on the doping concentration for one-photon absorption (the filled triangles) and two-photon absorption (the filled squares). Here, $T = 200$ K.
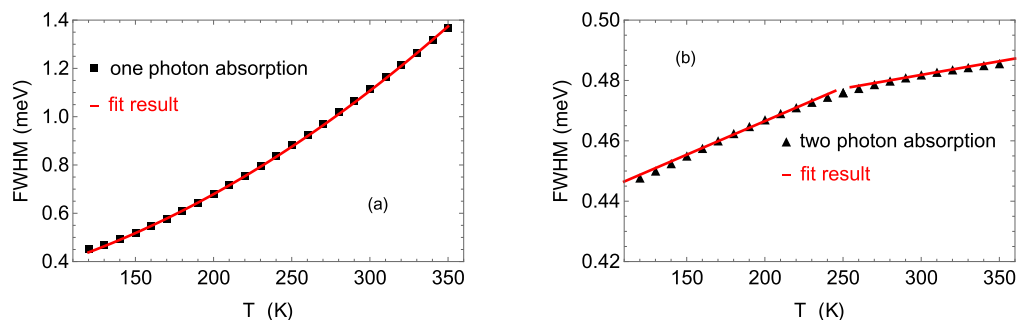

Fig. 6. The dependence of the FWHM on the temperature for one-photon absorption (a) and two-photon absorption (b). Here, $n_D = 10^{23}$ m^{-3}.

Acknowledgments

References

[1] L. Esaki, R. Tsu, IBM J. Res. Dev. 14 (1970) 61.
[2] M. Yarmohammadi, Phys. Lett. 380 (48) (2016) 4062.
[3] M. Yarmohammadi, J. Electron. Mater. 45 (10) (2016) 4958.
[4] H.D. Bui, M. Yarmohammadi, Superlattice. Microst. 122 (2018) 453.
[5] M. Yarmohammadi, H.A. Kazzaz, M.S. Feali, Int. J. Mod. Phys. B 31 (8) (2017) 1750045.
[6] G.H. Dohler, J.N. Miller, R.A. Street, P.P. Ruden, Surf. Sci. 174 (1986) 240.
[7] G.H. Dohler, H. Kunzel, K. Ploog, Phys. Rev. B 25 (4) (1982) 2616.
[8] S. Bhattacharya, D. De, S.M. Adhikari, K.P. Ghatak, Superlattice. Microst. 51 (2012) 203.
[9] C. V Nguyen, N.N. Hieu, Muoi Do, C.A. Duque, E. Feddi, H.V. Nguyen, L.T.T. Phuong, B.D. Hoi, H.V. Phuc, J. Appl. Phys. 123 (2018), 034301.
[10] L.T. T Phuong, T.C. Phong, M. Yarmohammadi, Sci. Rep. 10 (2020) 9201.
[11] B.D. Hoi, L.T.T. Phuong, T.C. Phong, J. Appl. Phys. 123 (2018), 094303.
[12] D.Q. Khoa, M. Davoudiniya, B.D. Hoi, M. Yarmohammadi, RSC Adv 9 (2019) 19006.
[13] D. Muoi, N.N. Hieu, C.V. Nguyen, B.D. Hoi, H.V. Nguyen, N.D. Hien, Nikolai A. Poklonski, S.S. Kubakaddi, H.V. Phuc, Phys. Rev. B 101 (2020) 205408.
[14] P.D. Khang, M. Davoudiniya, L.T.T. Phuong, T.C. Phong, M. Yarmohammadi, Phys. Chem. Chem. Phys. 21 (2019) 15133.
[15] N.V.Q. Binh, B.D. Hoi, D.V. Thuan, N.N. Hieu, C.V. Nguyen, H.V. Phuc, T.S. Tien, N.T.T. Nhan, N.D. Hien, N.N. Anh, L.T. Dung, L.T.T. Phuong, J. Phys. Chem. Solid. 125 (2019) 74.
[16] M. Yarmohammadi, M. Mortezaei Nobahari, T.S. Tien, L.T.T. Phuong, J. Phys. Condens. Matter 32 (2020) 465301.
[17] M. Yarmohammadi, M.R. Ebrahimi, Phys. Rev. B 100 (16) (2019) 165409.
[18] M. Yarmohammadi, AIP Adv. 6 (8) (2016) 085008.
[19] V.V. Bryskin, Yu A. Firsov, Zh. Eksp, Teor. Fiz 88 (1971) [Sov. Phys. JETP 61 (1971) 2373].
[20] A. Kastalsky, F.M. Peeters, W.K. Chan, L.T. Florez, J.P. Harbison, Appl. Phys. Lett. 59 (1991) 1708.
[21] S.G. Yu, V.B. Pevzner, K.W. Kim, M.A. Stroscio, Phys. Rev. B 58 (1998) 3580.
[22] S.C. Lee, J.W. Kang, H.S. Ahn, M. Yang, N.L. Kang, S.W. Kim, Physica E 28 (2005) 402.
[23] L.T.T. Phuong, H.V. Phuc, T.C. Phong, Comput. Mater. Sci. 49 (2010) S260.
[24] L.T.T. Phuong, H.V. Phuc, T.C. Phong, Physica E 56 (2014) 102.
[25] B.D. Hoi, L.T.T. Phuong, T.C. Phong, Superlattice. Microst. 100 (2016) 365.
[26] D.Q. Khoa, L.T.T. Phuong, B.D. Hoi, Superlattice. Microst. 103 (2017) 252.

[27] K. Ploog, G.H. Dohler, Adv. Phys. 32 (3) (1983) 285.
[28] Sam Nyung YiaJong June SongbKyu Soon BaebSang Don Choi, Phys. B Condens. Matter 222 (1996) 209.
[29] Nam Lyong Kang, Sang Don Choi, J. Phys. Soc. Jpn. 78 (2009), 024710.
[30] Hyun Jung Lee, Nam Lyong Kang, Joung Young Sug, Sang Don Choi, Phys. Rev. B 65 (2002) 195113.
[31] Nam Lyong Kang, Hyun Jung Lee, Sang Don Choi, J. Kor. Phys. Soc. 44 (4) (2004) 938.
[32] A. Michael, Stroscio, Phys. Rev. B 40 (1989) 6428.
[33] M. Masale, N.C. Constantinou, Phys. Rev. B 48 (1993) 11128.
[34] Y. He, Z. Yin, M.S. Zhang, T. Lu, Y. Zheng, Mater. Sci. Eng. B 75 (2000) 130.
[35] N. Mori, H. Momose, C. Hamaguchi, Phys. Rev. B 45 (1992) 4536.